THE ASTROPHYSICAL JOURNAL, 404:663–672, 1993 February 20

EXTREME ULTRAVIOLET OBSERVATIONS OF G191-B2B AND THE LOCAL INTERSTELLAR MEDIUM WITH THE HOPKINS ULTRAVIOLET TELESCOPE

RANDY A. KIMBLE,[1] ARTHUR F. DAVIDSEN,[2] WILLIAM P. BLAIR,[2] CHARLES W. BOWERS,[2] W. VAN DYKE DIXON,[2] SAMUEL T. DURRANCE,[2] PAUL D. FELDMAN,[2] HENRY C. FERGUSON,[3] RICHARD C. HENRY,[2] GERARD A. KRISS,[2] JEFFREY W. KRUK,[2] KNOX S. LONG,[4] H. WARREN MOOS,[2] AND OLAF VANCURA[2]

Received 1992 May 19; accepted 1992 August 20

ABSTRACT

During the *Astro-1* mission in 1990 December, the Hopkins Ultraviolet Telescope (HUT) was used to observe the extreme ultraviolet spectrum (415–912 Å) of the hot DA white dwarf G191-B2B. Absorption by neutral helium shortward of the 504 Å He I absorption edge is clearly detected in the raw spectrum. Model fits to the observed spectrum require interstellar neutral helium and neutral hydrogen column densities of $1.45 \pm 0.065 \times 10^{17}$ cm^{-2} and $1.69 \pm 0.12 \times 10^{18}$ cm^{-2}, respectively. Comparison of the neutral columns yields a direct assessment of the ionization state of the local interstellar cloud surrounding the Sun. The neutral hydrogen to helium ratio of 11.6 ± 1.0 observed by HUT, like the lower signal-to-noise results of a similar measurement by Green, Jelinsky, & Bowyer (1990b), strongly contradicts the widespread view that hydrogen is much more ionized than helium in the local interstellar medium, a view which has motivated some exotic theoretical explanations for the supposed high ionization.

In fact, the HUT observation implies somewhat greater ionization of helium than hydrogen in the local cloud, consistent with models of the local cloud based on known sources of ionization. Consistency with solar radiation backscatter measurements can be achieved if a neutral hydrogen attenuation mechanism such as the charge-exchange proposed by Ripken & Fahr (1983) operates at the heliopause. In that case, adjusting the typical backscatter-derived local densities for such an effect, we find that within the local cloud the particle densities are $n_{\rm H} \simeq 0.13$–0.15 cm^{-3}, $n_{\rm He} \simeq 0.013$–0.015 cm^{-3}, and $n_e \simeq 0.03$ cm^{-3}; the ionized fractions are $X_{\rm H} \simeq 0.1$–0.2 and $X_{\rm He} \simeq 0.1$–0.35; the total hydrogen column density of the local cloud toward G191-B2B is $\sim 2.2 \times 10^{18}$ cm^{-2}; and the cloud extends ~ 5 pc in that direction.

Subject headings: ISM: abundances — stars: individual (G191-B2B) — ultraviolet: stars

1. INTRODUCTION

The Hopkins Ultraviolet Telescope (HUT), which flew aboard the space shuttle Columbia as part of the *Astro-1* mission in 1990 December, was developed primarily for spectrophotometric observations in the 912–1850 Å range of the far ultraviolet (Davidsen et al. 1992). However, the same design features which provide good performance for HUT down to 912 Å also yield significant effective area in the 415–912 Å range of the extreme ultraviolet (Davidsen et al. 1991a). These wavelengths of course lie in the heart of the Lyman continuum of hydrogen; the photoelectric opacity of neutral hydrogen, which precludes observation of distant sources at these wavelengths, provides the very definition of the astronomical EUV. In addition, this range contains the resonance lines and ionization edge (at 504 Å) of neutral helium, which, despite its high cosmic abundance, is virtually impossible to detect in the interstellar medium at any other wavelength. In this work, we use the unique EUV capabilities provided by HUT to carry out an absorption study of the local interstellar medium.

The local interstellar medium (LISM) is the region within roughly 100 pc of the Sun. An excellent review of the properties of this region has been presented by Cox & Reynolds (1978). Of greatest interest for the present purpose are two key points. First, over distances which vary from direction to direction, but which are characteristically of order 100 pc, the LISM is essentially devoid of neutral material. Instead it is filled largely with tenuous 10^6 K gas whose thermal emissions give rise to much of the soft X-ray background. Second, despite the dominance of million degree gas within this local bubble, the Sun itself happens to lie within a much cooler, at least partly neutral cloudlet sometimes referred to as the "local fluff." Observations of the backscattering of solar resonance line radiation from interstellar gas flowing through the solar system imply a neutral hydrogen density of $n_{\rm H\,I} \sim 0.05$–0.10 cm^{-3} and a temperature of ~ 8000 K for this material (e.g., Bertaux et al. 1985; Chassefière et al. 1986). Complementary to these point measurements of the properties of the local cloudlet are hydrogen column density determinations made along the line of sight to nearby stars; the low H I columns derived ($\sim 10^{18}$ cm^{-2}) imply that the local fluff extends only ~ 3 to 6 pc in most directions before the hot, fully ionized medium is encountered (cf. Bruhweiler & Vidal-Madjar 1987).

It is this local cloud whose properties we will investigate by means of EUV absorption measurements with HUT. Specifically, we will address the question of the ionization state of the very local material. The ionization question is troubling because several lines of observational evidence have suggested a much higher hydrogen ionization fraction in the local cloud than can be maintained by known sources of ionization in the LISM. Because of the intimate connection between the proper-

[1] Laboratory for Astronomy and Solar Physics, Code 681, NASA/Goddard Space Flight Center, Greenbelt, MD 20771.
[2] Department of Physics and Astronomy, The Johns Hopkins University, Charles & 34th Streets, Baltimore, MD 21218.
[3] Institute of Astronomy, University of Cambridge, The Observatories, Madingley Road, Cambridge, CB3 0HA, England.
[4] Space Telescope Science Institute, 3700 San Martin Drive, Baltimore, MD 21218.

ties of the local cloud and the contents, properties, and history of the larger scale LISM, the ionization question takes on a significance beyond a purely parochial interest in our very local habitat in the Galaxy.

Observations of the EUV continuum spectra of targets outside the local cloud can help resolve this controversy. By measuring the degree of attentuation of the EUV spectrum in the Lyman continuum, the neutral hydrogen column density through the local cloud can be determined along a particular line of sight; similarly, the strength of the He I absorption edge at 504 Å provides a measurement of the neutral helium column through the same material. Comparison of the neutral columns to the relative cosmic abundance of hydrogen and helium then yields a direct determination of the relative ionization of the two species.

A pioneering measurement of this kind has been made with a sounding rocket experiment by Green, Jelinsky, & Bowyer (1990b, hereafter GJB). From their observation, GJB claimed the first detection of interstellar absorption at the He I 504 Å edge, though the low signal-to-noise ratio data obtainable in a rocket flight permitted a rather wide range of column densities and relative ionization. In this paper, we describe a much more precise measurement carried out with the Hopkins Ultraviolet Telescope, using the same background source, the hot DA white dwarf G191-B2B.

2. OBSERVATIONS

The Hopkins Ultraviolet Telescope comprises a 0.9 m primary mirror feeding a prime focus, Rowland circle spectrograph (Davidsen et al. 1992). The dispersed photons are imaged onto a photon-counting microchannel-plate detector coupled to a phosphor screen and one-dimensional Reticon-diode-array readout. First-order spectra cover the spectral range 830–1860 Å with a sampling of 0.51 Å per pixel and a point source resolution of ~3 Å. For those targets (such as G191-B2B) whose sub–912 Å flux is not completely cut off by interstellar hydrogen absorption, EUV spectra from higher grating orders overlap the first-order far-ultraviolet spectrum. A thin-film aluminum filter mounted on the spectrograph's slit wheel can be interposed to reject the first-order FUV radiation, providing a pure EUV bandpass from about 350 to 700 Å. A rapid drop in throughput at short wavelengths due to the two normal incidence reflections in the instrument prevents wavelengths below about 350 Å in higher grating orders from contributing significantly to the total spectrum.

We observed G191-B2B with HUT on 1990 December 5. The target was observed first with no filter for 366 s and then through the aluminum EUV filter for an additional 1140 s. The unfiltered spectrum was obtained during orbital night, where minimum airflow contamination of the spectrum is encountered. All but the final 200 s of the filtered spectrum were also obtained during orbital night. By far the brightest dayglow line expected in the aluminum filter bandpass is the 584 Å resonance line of He I. This line is present at only the 2 σ level despite lying in a very low count region of the total filtered spectrum, indicating that airglow emissions contribute negligibly to the total observed EUV spectrum.

Both the unfiltered and filtered spectra of G191-B2B were taken through 30″ circular apertures. Despite problems encountered with the Spacelab Instrument Pointing System, the Payload Specialist on board was able to guide the pointing manually, using guide stars in the field of the HUT TV camera which views the focal plane. For the unfiltered observation, the high count rate (2600 counts s^{-1}) yields good photometric precision in each of the 2 s intervals at which data were telemetered to the ground; frames in which significant pointing jitter took even a small portion of the signal outside the entrance slit were thus easily flagged and removed. Only three such frames were seen (totalling 6 s—less than 2% of the unfiltered observation time). Only a small portion of the signal was lost for even these frames, so that had they been included, a negligible error (<0.3%) would have resulted in the photometry. This conclusion is important because the low count rate in the filtered EUV spectrum (~15 counts s^{-1}) does not provide high-precision confirmation of the pointing over short time intervals. No long-term drifts in the filtered spectrum count rate are seen, however, and the pointing errors determined from the positions of the guide stars in the HUT TV camera are as small as for the unfiltered spectrum. We conclude that the filtered spectrum is also photometrically accurate. Miscentering of the target within the large aperture can shift the wavelength scale of the acquired spectrum slightly. (The 30″ aperture width corresponds to 10 Å in first order and 5 Å in second order.) We therefore have used stellar spectral features (the Lyman series in the unfiltered FUV spectrum and the He I 504 Å edge itself in the filtered EUV spectrum) to determine the small offsets from the nominal HUT wavelength calibration.

The HUT EUV spectrum obtained for G191-B2B is shown in Figure 1. (The unfiltered FUV spectrum of G191-B2B is presented in Davidsen et al. 1992.) The data shown are the raw count data, binned by 4 pixels to yield 1.027 Å spectral bins in second order, and plotted against the second-order wavelength for each bin; higher grating orders also contribute to the total spectrum at the long-wavelength end of the detector. Sharp drops in the observed spectrum are seen at 504 Å in both second and third order, indicating strong detection of the He I absorption edge in the raw data. The steep decline seen longward of the 504 Å edge represents the combined effects of increasing H I photospheric opacity, increasing H I interstellar opacity, and falling transmission of the aluminum filter.

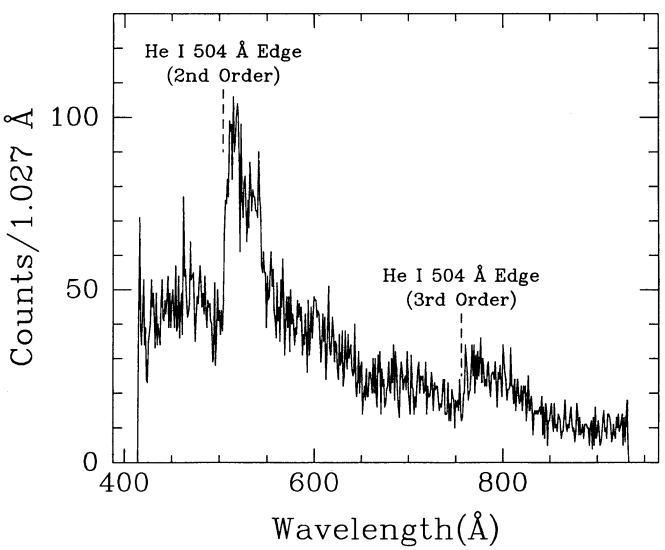

FIG. 1.—The EUV (raw) count spectrum of G191-B2B obtained by the Hopkins Ultraviolet Telescope. The abscissa is labeled with the second-order wavelength corresponding to each spectral bin, though third-order wavelengths contribute significantly to the observed spectrum at the long-wavelength end of the detector. Absorption by interstellar helium shortward of its absorption edge at 504 Å is clearly visible in both second and third order in the raw data.

As noted above, the sounding rocket experiment of GJB obtained a rather low signal-to-noise ratio EUV spectrum of G191-B2B. Hence, their analysis required model fitting of the spectrum far away from 504 Å in order to obtain a statistically significant detection of the edge, introducing far greater susceptibility to calibration or model atmosphere uncertainties than will be the case for analysis of the HUT data. The HUT spectrum shown here thus represents the first unambiguous, high-significance detection of He I absorption in the local interstellar medium.

3. DATA REDUCTION AND ANALYSIS

Our derivation of the neutral hydrogen column density toward G191-B2B is based on a comparison between the flux observed from the star just longward of 504 Å with the flux predicted by a model atmosphere calculation. The accuracy of the hydrogen column measurement thus depends (logarithmically) on the accuracy of both the instrumental calibration and the model atmosphere prediction. The helium column determination, in contrast, is insensitive to the absolute values of these parameters, as it is measured from the observed jump across the 504 Å absorption edge.

There are no absolute standards available for in-flight calibration at 500 Å. Accordingly, we have taken considerable pains to determine the instrumental throughput from a combination of pre- and postflight laboratory calibrations and a comparison of those results with in-flight calibration longward of 912 Å. The details of the procedures are likely not of general interest; however, given the relative novelty of observations in this wavelength range, we provide a thorough discussion of the instrumental calibration in the Appendix. The significant conclusion, drawn from the striking confirmation of the laboratory calibration by the in-flight FUV calibration, is that the adopted instrumental sensitivity near 504 Å is accurate to within $\sim 10\%$.

Uncertainty in the model atmosphere–predicted flux near 504 Å for G191-B2B is at a similar level. In performing the model fitting, we use a pure hydrogen model atmosphere for G191-B2B, kindly provided by P. Bergeron. The model atmosphere calculation uses the effective temperature (59,250 $\pm$ 2000 K) and gravity ($\log g = 7.5$) determined from Balmer line profile fitting by K. Kidder (unpublished), as cited by Holberg et al. (1991), normalized to a V magnitude of 11.78. The ± 2000 K effective temperature uncertainty corresponds to $\pm 10\%$ uncertainty in the true stellar flux in the 504 Å region, assuming a pure hydrogen atmosphere.

In addition, it is well known that *EXOSAT* observations of this and other DA white dwarfs in the 80–200 Å range imply the presence of some other opacity source besides hydrogen in the stellar atmosphere to suppress the flux below pure hydrogen model predictions. Hence, some remarks about the significance of potential compositional uncertainties are in order. The broad-band flux deficit for G191-B2B in the *EXOSAT* range (no *EXOSAT* grating spectrum was ever obtained) has been ascribed by various authors to several possible sources: opacity due to helium, either mixed homogeneously with the hydrogen (Paerels & Heise 1989) or lying below a thin hydrogen envelope in a stratified atmosphere (Koester 1989), or opacity due to line blanketing from trace metals in the photosphere (Vennes et al. 1992), a mechanism required to explain the peculiar *EXOSAT* grating spectrum of another hot DA, Feige 24 (Vennes et al. 1989).

Fortunately, none of these potential means of suppressing the short-wavelength flux significantly affects the emergent flux near the 504 Å edge. Those homogeneous hydrogen/helium atmospheres and stratified hydrogen over helium atmospheres that are consistent with the Balmer line profiles observed by Finley & Koester (1992) differ from pure hydrogen models by less than 3% in the critical 504 Å region. In addition, *no* intrinsic He I edge is present in homogeneous or stratified model atmospheres which are consistent with the *absence* of He II Balmer lines in the HUT FUV spectrum. A full discussion of HUT constraints on such atmospheres will be presented in a separate paper (Kimble et al. 1992a). Model calculations by Vennes et al. (1992) which include iron opacity at a level consistent with the presence of iron lines in high-dispersion *IUE* spectra (Bruhweiler & Feibelman 1992) and FOS spectra (Sion et al. 1992) do show noticeable accumulated effects in the mid-EUV, but not at a strong level. The iron opacity in the EUV spectrum predicted by Vennes et al. (1992) produces less than 3% total blanketing in the 479–504 Å and 504–529 Å ranges. We conclude therefore that the use of a pure hydrogen atmosphere does not influence our results in a significant way.

With the instrumental calibration and model atmosphere in hand, we fit to the observed spectrum in order to derive the interstellar absorbing column densities. We restrict the model fitting to a narrow region (± 25 Å) around the 504 Å edge. It is desirable to keep the interval as narrow as possible to minimize any model- and calibration-dependent effects in measuring the edge strength. Near the second-order 504 Å edge, the less well-determined third-order contribution to the observed spectrum is small (see Appendix), whereas at longer wavelengths, the contribution of the third-order signal grows rapidly. By second-order 650 Å, third order clearly dominates the total observed spectrum. At shorter second-order wavelengths, calibration and model flux uncertainties also grow. The ± 25 Å range employed provides ample statistical precision in the results, which are not sensitive to small changes in the wavelength interval used.

In carrying out the model fitting, we take the observed spectrum to be comprised of the stellar second-order signal, the stellar third-order signal, detector background (determined in-flight from closed slit integrations), and grating scattered light. Free parameters in the fit are the neutral hydrogen and helium absorbing columns, a linear shift in the nominal wavelength scale (to allow for miscentering of the target within the 30″ aperture), and a Gaussian instrumental point-spread function to take into account both the intrinsic resolution of the spectrograph and blurring of the resolution due to pointing jitter within the slit. Neither of these last two parameters significantly affects the best-fitting column density results.

We take into account also the continuum opacity of the residual terrestrial atmosphere above the 358 km altitude of the shuttle. In deriving the small (9%) correction to the observed flux, we utilize the MSIS-86 thermospheric model of Hedin (1987), referenced to the solar $F_{10.7}$ flux and the local time appropriate to the observation.

For the neutral hydrogen absorption cross section, we use the standard analytic function (e.g., Spitzer 1978) which can be derived rigorously from quantum physics. For neutral helium, we use the analytic approximation presented by Koester et al. (1985), which agrees to within 2% at the relevant wavelengths with the composite laboratory determinations compiled by Marr & West (1976) and with the theoretical calculations of Reilman & Manson (1979). For normal cosmic abundances, the contributions of other elements to the total interstellar absorption in this wavelength region are completely negligible (Cruddace et al. 1974). With regard to the helium cross section,

we note that the values used in the oft-cited Cruddace et al. reference can be traced to a 1965 experiment (Lowry, Tomboulian, & Ederer 1965) whose results near the 504 Å edge are higher by approximately 10% than the modern values in the references cited above. This leads to helium column densities approximately 10% lower for a given strength of the 504 Å edge when the older cross section is used. We believe that GJB used these earlier cross sections in the analysis of their rocket data on G191-B2B; a systematic disagreement at the 10% level will thus be built into our analyses.

The resulting best fit to the HUT spectrum in the 479–529 Å region is shown in Figure 2. Contributions of the various orders and the detector background and scattered light are shown explicitly in the figure. The minimum χ^2 is 54.4 for 45 degrees of freedom, indicating an excellent fit to the data. The unattenuated model atmosphere flux at Earth and the flux after absorption by the best-fitting interstellar column densities are shown in Figure 3. The fluxes at Earth just above and just below the 504 Å edge are 4.29×10^{-12} ergs cm^{-2} s^{-1} Å^{-1} and 1.48×10^{-12} ergs cm^{-2} s^{-1} Å^{-1}, respectively. The best-fitting column densities and 1 σ statistical error bars are

$$N_{\rm H\,I} = 1.69 \pm 0.02 \times 10^{18}\ {\rm cm}^{-2}$$

$$N_{\rm He\,I} = 1.45 \pm 0.065 \times 10^{17}\ {\rm cm}^{-2}.$$

The 90% and 99% confidence intervals on the two columns considered jointly are shown in Figure 4. Also shown are the results derived by GJB.

The potential systematic uncertainties described above broaden the allowed range of neutral hydrogen columns somewhat beyond the purely statistical contours shown in Figure 4. As noted previously, the hydrogen column density is determined by the flux observed longward of 504 Å in comparison with the model atmosphere prediction. The best-fitting hydrogen column produces more than two optical depths of absorption in the region just longward of the 504 Å edge. Because of the logarithmic dependence of the derived column density on the observed versus unattenuated intensity ratio, a given percentage error in the instrumental calibration or model atmosphere flux leads to slightly less than half that error in the derived hydrogen column. The ±10% uncertainty in the instrumental sensitivity and the ±10% uncertainty in the model atmosphere flux combine in quadrature to yield a ±14% uncertainty in the observed versus unattenuated intensity ratio, and a ±7% uncertainty in the derived hydrogen column. We thus quote $1.69 \pm 0.12 \times 10^{18}$ cm^{-2} as the appropriate limits on the hydrogen column and note that the statistical contours shown in Figure 4 could shift by ±7% in hydrogen column due to these potential systematic effects.

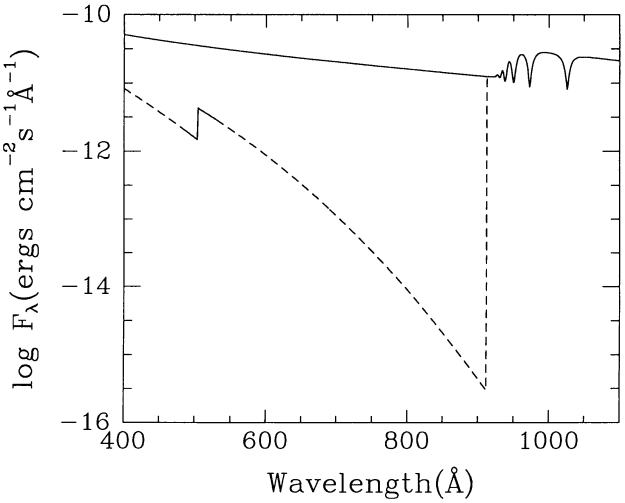

FIG. 3.—EUV flux at Earth from G191-B2B. The upper curve represents the flux predicted by the unattenuated pure hydrogen model atmosphere calculation. The lower curve shows the model flux after attenuation by the interstellar absorbing columns required to fit the HUT data. The solid portion of the lower curve indicates the wavelength region of the fit to the HUT spectrum, which thus constitutes a measurement of the flux at the plotted level over that interval. Toward longer wavelengths, potential metal opacity in the G191-B2B photosphere is not expected to substantially affect the flux, but order confusion prevents HUT from explicitly measuring the flux level. Toward shorter wavelengths, the spectrum presumably begins to deviate below the pure hydrogen prediction, according to broad-band *EXOSAT* measurements.

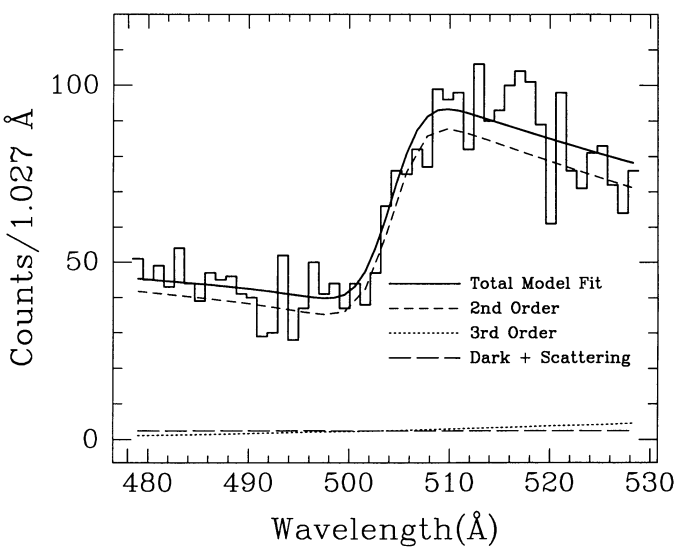

FIG. 2.—Model fitting to the observed EUV spectrum in the vicinity of the 504 Å helium absorption edge. The contributions of second and third grating orders, as well as instrumental dark count and scattered light, are indicated. The model fit leads to well-determined values for the interstellar neutral helium and neutral hydrogen column densities along the line of sight to G191-B2B.

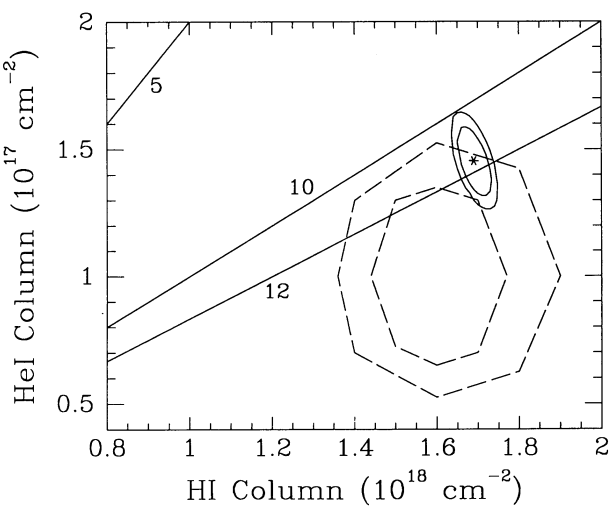

FIG. 4.—Joint confidence contours on the interstellar neutral hydrogen and helium columns toward G191-B2B. The dashed contours are the 90% and 99% confidence limits of Green, Jelinsky, & Bowyer (1990b). The solid contours are the 90% and 99% confidence limits from our analysis of the HUT spectrum. Lines of constant neutral hydrogen to helium ratio are also indicated: 5 (an oft-cited value for the neutral ratio in the local ISM, ruled out by the GJB and HUT results), 10 (the canonical cosmic abundance ratio), and 12.

The helium column, on the other hand, is derived from the fractional drop in the observed intensity across the 504 Å edge. It is thus unaffected to first order by errors in the overall level of the instrumental calibration or model flux. It is sensitive instead only to *relative* errors across the narrow wavelength interval used in the fitting. The model atmosphere slope across this interval varies by only 1% over the possible temperature range, so no additional broadening of the error bar on the helium column is required.

Before proceeding with a discussion of the column density results, we turn briefly to a completely separate issue which can be addressed by the HUT EUV observation of G191-B2B. From their sounding rocket observation of G191-B2B, Green, Bowyer, & Jelinsky (1990a) also claimed a weak (3.8 σ) detection of 584 Å line emission from G191-B2B or its vicinity (within their 2′ diameter entrance aperture), at a level well in excess of expected geocoronal or interplanetary 584 Å background levels. Their reported flux was 0.67 photons cm^{-2} s^{-1}. Green et al. (1990a) considered as possible sources of the signal both chromospheric emission from the cool star companion G191-B2A and recombination emission from a small ($\sim$10 AU in radius) photoionized nebula surrounding G191-B2B itself, though they did not find the required parameters for either interpretation particularly plausible.

No such strong line emission is visible in the HUT spectrum (see Fig. 1). A feature at the 2 σ level is present, with a flux of 0.035 ± 0.016 photons cm^{-2} s^{-1}, far below the flux reported by Green et al. (1990a), and consistent with airglow emission. We conclude that no such 584 Å emission is present in G191-B2B or a surrounding nebula. However, the cool companion G191-B2A was not within the smaller entrance slit of the HUT observation; hence, if real, the emission presumably arises from that source.

4. DISCUSSION

The HUT EUV observations yield accurate determinations of both the neutral hydrogen and neutral helium interstellar absorbing columns along the line of sight to G191-B2B. As Figure 4 indicates, the derived columns differ (by 6% for $N_{\rm H\,I}$ and by nearly 50% for $N_{\rm He\,I}$) from the best-fitting parameters of GJB, but the more precise HUT results do overlap the 99% contours of that rocket experiment. Reasonable agreement with previous estimates of the H I column is found as well. Bruhweiler & Kondo (1982) estimated $N_{\rm H\,I} \sim 8.3 \times 10^{17}$ cm^{-2} on the basis of scaling from interstellar N I lines. Jelinsky, Bowyer, & Basri (1988) derived $N_{\rm H\,I} = 0.6\text{–}5.2 \times 10^{18}$ cm^{-2} from a similar analysis; their wide range indicates the level of uncertainty which can be expected from the N I scaling arguments. Paerels & Heise (1989) derived $N_{\rm H\,I} > 1.5 \times 10^{18}$ cm^{-2} from model fitting to *EXOSAT* photometry; however, given the likelihood that metal opacity in the G191-B2B photosphere is important in the *EXOSAT* range (as discussed above), the significance of the fit to a homogeneous hydrogen and helium atmosphere is not clear for the X-ray data. Finally, Holberg (1984) derived $N_{\rm H\,I} = 1.0 \times 10^{18}$ cm^{-2} from observations longward of 500 Å by the *Voyager* UV spectrometers; no estimate of the uncertainty was given.

The HUT EUV observation of G191-B2B provides the first precise determinations of both the neutral hydrogen and neutral helium column densities along any line of sight through the LISM. This combination offers a unique opportunity to assess directly the ionization state of this material. We now explore the ramifications of the G191-B2B observation in that regard.

It is important to consider what interstellar material the absorption measurement is probing. G191-B2B lies at a distance of 48 pc (Routly 1972) toward Galactic coordinates $l = 155\overset{\circ}{.}9$ and $b = 7\overset{\circ}{.}1$. The line of sight presumably passes mostly through the 10^6 K gas thought to fill most of the local bubble (cf. Cox & Reynolds 1987). The hot, low-density material contributes negligibly to the neutral absorbing columns. Instead, the neutral columns must arise from cooler, denser regions of interstellar gas along the line of sight. As noted above, the Sun is known to be located within just such a condensation. Furthermore, the H I column densities to much nearer stars typically lie in the $1\text{–}2 \times 10^{18}$ cm^{-2} range (cf. Bruhweiler & Vidal-Madjar 1987), indicating that H I columns similar to that observed toward G191-B2B are encountered entirely within the local cloudlet. (With the usually estimated local cloudlet density of $n_{\rm H\,I} = 0.05\text{–}0.10$ cm^{-3}, a path length of 5–11 pc is required to yield the observed G191-B2B H I column.) As pointed out by GJB, the nearby star Capella ($d = 14$ pc) offers a particularly valuable comparison, as it lies only 8° away from G191-B2B, so that its line of sight presumably probes very similar local cloud material. Linsky et al. (1993) have recently used high-resolution Lyman-α observations of Capella with the *Hubble Space Telescope* to determine an H I column of $1.8^{+0.3}_{-0.1} \times 10^{18}$ cm^{-2}. The close similarity to the $1.69 \pm 0.12 \times 10^{18}$ cm^{-2} HUT column toward G191-B2B reinforces the conclusion that the neutral columns toward the more distant star do arise entirely within the local cloudlet, and that it is the ionization state of this very local material which we are examining.

The HUT measurements of the absorbing columns yield an interstellar neutral hydrogen to neutral helium ratio of 11.6 ± 1.0. The uncertainty quoted here combines the 1 σ statistical error bar derived from the model fitting in quadrature with the $\pm 7\%$ potential systematic uncertainty in the neutral hydrogen column described above.

Of course, inferring the relative ionization of the two species from their *neutral* column ratios requires knowledge of the *total* abundance ratio in the local interstellar medium. This ratio itself is uncertain at approximately the 10% level. Aller (1987) has reviewed abundance determinations from observations of H II regions and planetary nebulae and concluded that H/He = 10. (This canonical hydrogen to helium ratio is indicated as a line in Fig. 4). One commonly cited H II region study supporting this value is the work of Peimbert et al. (1988) on the Orion Nebula. However, the recent work of Baldwin et al. (1991) argues that a more detailed analysis of the Orion Nebula yields $H/He = 11.4 \pm 0.8$.

Unfortunately, direct measurements in the solar system offer little aid. The helium resonance lines lie in the difficult-to-observe ultraviolet. Because of their high excitation energies, they arise only in the difficult-to-model active outer regions of the Sun rather than in the solar photosphere. The chondritic meteorites used for deriving solar system heavy element abundances, on the other hand, do not retain volatiles such as helium. One approach which does yield results on the solar system helium abundance is the construction of solar models. These models, constrained by the age of the solar system, solar luminosity, and heavy element abundance, imply a primordial solar helium abundance. In a recent example of such modeling, Turck-Chieze et al. (1988) derive a primordial solar abundance ratio of $H/He = 10.1 \pm 0.7$.

The HUT neutral hydrogen–to–helium ratio for the local interstellar cloud is thus quite close to the total cosmic abundance ratio; exact agreement is within the combined uncer-

tainties. The best-fitting values, however, indicate a slightly higher neutral H/He ratio than the total cosmic ratio, implying a higher fractional ionization for helium than for hydrogen in the local cloud. In either case, the HUT G191-B2B absorption measurements strongly contradict the widespread view (cf. Bertaux et al. 1985) that hydrogen is preferentially ionized in the local cloud, with a neutral density ratio H/He $\sim$ 5. (A line representing a neutral column ratio of 5 is shown in Fig. 4.)

The same conclusion excluding preferential ionization of hydrogen was reached by GJB from their EUV absorption measurement. However, as shown in Figure 4, the GJB results would allow strong preferential ionization of helium; the HUT data rule out that possibility as well.

The tight constraints on the local neutral hydrogen–to-helium ratio, and in particular the rejection of preferential hydrogen ionization in the local cloud, are the principal conclusions of our analysis. In order to place their significance in context, in the following we (1) outline the arguments that led in the first place to the common (though not universal) view that hydrogen is preferentially ionized in the local cloud, (2) point out the difficulties that were encountered in trying to produce a high hydrogen ionization fraction with known ionizing sources, (3) note some of the dramatic explanations that were advanced to account for the conflicting observations, and finally (4) indicate the likely means by which the disparate pieces of observational data can be reconciled.

The most direct observational evidence in favor of a low neutral H/He ratio locally (preferential ionization of hydrogen) has come from solar system backscatter measurements. In this technique (e.g., Bertaux et al. 1985; Chassefière et al. 1986), model fitting to maps of the intensity of the backscattering of solar resonance lines (H I λ1216 and He I λ584) by interstellar gas atoms flowing through the solar system permits a determination of the gas density and temperature, as well as the direction of motion of the Sun with respect to the local interstellar material. The modeling is complex, and the results depend directly on accurate knowledge of the solar line flux as well as the instrumental calibrations. As a result, the densities derived from different experiments range over at least a factor of 2, and any single determination of a low neutral H/He ratio might be accorded little weight. However, considered collectively (see Cox & Reynolds 1987 for a compilation of results to that time), the backscatter data provide very suggestive evidence that, *at least within the solar system*, the neutral H/He ratio in the interstellar gas lies significantly below the total cosmic abundance ratio. Taken at face value, the observed neutral H/He ratio implies a hydrogen ionization fraction of 0.3–0.7 if the helium is completely neutral and higher if the helium is also ionized. (The qualification "*within the solar system*" foreshadows what will be offered as the likely source of systematic error in the backscatter data.) The typical local densities derived are $n_{\rm H\,I} \simeq 0.05$ cm^{-3} and $n_{\rm He\,I} \simeq 0.01$ cm^{-3}.

Estimates of the electron density in the local cloud can be made by comparing absorption-line determinations of Mg I and Mg II column densities, since the relative densities of these two ionization stages can be related to the total electron density through the standard ionization/recombination equilibrium equation. In this manner, Cox & Reynolds (1987) have used the $N_{\rm Mg\,I}/N_{\rm Mg\,II}$ ratios observed by Bruhweiler et al. (1984) to infer a local electron density of 0.026–0.10 cm^{-3}. As this value is comparable to the neutral hydrogen number density found from the backscatter experiments, a substantial ionzation fraction for hydrogen is often inferred.

Finally, for the hot DA white dwarfs HZ 43 and GD 153, the interstellar absorbing columns derived from *EXOSAT* observations are found to be incompatible with (i.e., higher than) the columns required to fit the EUV observations of those stars with *Voyager* longward of 500 Å. Since neutral helium contributes significantly to the total opacity at *EXOSAT* wavelengths, but not at all in the *Voyager* range, it was pointed out (Paerels et al. 1986; Heise et al. 1988; Paerels & Heise 1989) that the disparate columns could be reconciled if the hydrogen along the line of sight to these stars were substantially ionized, while the helium remained neutral. Just as for the individual backscatter experiments, no single one of these arguments for high ionization of hydrogen is unassailable. However, taken together, arguments like these led to the common belief that a high local ionization fraction of hydrogen, significantly greater than that of helium, had been observationally established.

The problem lies in accounting for the supposed high hydrogen ionization fraction with known ionizing sources. Models of the local cloud have been constructed including ionization by cosmic rays, the soft X-ray background, known and extrapolated stellar EUV sources, and EUV ionizing radiation from the local bubble (Cheng & Bruhweiler 1990), as well as from the putative conductive interface between the local cloudlet and the surrounding coronal gas (Slavin 1989). The ranges of parameters considered invariabily lead to too little hydrogen ionization within the cloud, with a typical ionization fraction $X_{\rm H}\,[= n_{\rm H\,II}/(n_{\rm H\,I} + n_{\rm H\,II})]$ of 0.2. Note that the quadratic dependence of the equilibrium ionization rate on the ionized particle density makes the disagreement larger than it might appear at first glance. For a given observed neutral hydrogen density, the ionization rate required to achieve an equilibrium ionization fraction of 0.5 is 16 times larger than that required to sustain the ionization fraction of 0.2 found in the models. In addition, the local cloud models actually predict somewhat greater ionization of helium than hydrogen within the cloud (Cheng & Bruhweiler 1990; Slavin 1989), exacerbating the discrepancy with the backscatter results.

The marked discrepancy between the model-predicted ionization state of the local interstellar cloud and the ionization state which had been inferred from previous observations can in principle be resolved in at least two different ways: either by postulating a heretofore unknown source of ionizing flux far more intense than known sources, or by dropping the equilibrium assumption in the ionization calculation. Both explanations have been advanced, and both carry significance beyond a simple understanding of our very local cloud. The supposed need for a new source of ionization to account for the observations of the local cloud has been used by Sciama (1991) as one of several motivations for his comprehensive model, enunciated in a series of papers, in which hydrogen-ionizing photons from the decay of massive neutrinos in both Galactic halos and the intergalactic medium produce ionization in a wide range of astrophysical environments. These decay photons have wavelengths just below 912 Å and thus can ionize hydrogen but not helium, as demanded by the backscatter observations. The absence of any such neutrino decay signature in the HUT observations of the rich galaxy cluster Abell 665 has, however, strongly contradicted the basic assumptions of this model (Davidsen et al. 1991b); radiative neutrino decay at a rate consistent with the HUT limits would not contribute significantly to ionization of the LISM.

The alternative explanation, that the local cloud is not in ionization equilibrium, is not unreasonable. The recombination time scale for gas with a density of 0.1 cm^{-3} and temperature near 10^4 K is long ($\sim 10^6$ yr). Hence, if a supernova

had ionized the local cloud relatively recently, its current state of ionization would not represent equilibrium with the remaining ionizing sources within the local bubble. While not requiring new physics like the Sciama interpretation, the conclusion that a supernova had occurred quite recently in the local bubble would still be a dramatic deduction from observations of the ionzation of our local cloud. It would help greatly in discriminating between possible models for the local bubble (see Cox & Reynolds 1987 for an extensive discussion). One model relies on just such a recent supernova to create the local bubble which would thus still be expanding; alternatively, the local bubble may be a longer lived structure created as much as 10^7 yr ago by a collection of supernovae and now in pressure equilibrium with its surroundings.

We find, however, that the seeming discrepancy between the observed and predicted ionization state of the local cloud is not real, and thus dramatic steps to account for the discrepancy are completely unnecessary. The neutral hydrogen–to-helium ratio of 11.6 ± 1.0 along the line of sight through the local cloud to G191-B2B is in good agreement with the modest preferential ionization of helium that results from ionizing line radiation from the local bubble in the models of Cheng & Bruhweiler (1990) and Slavin (1989). In "model C" of Cheng & Bruhweiler, for example, the ratio of neutral column densities as observed from the center of the local cloud to the edge is 11.5 for a cosmic abundance ratio of 10, in excellent agreement with the HUT result. Figure 5 presents the HUT constraints on the ionization fractions of hydrogen and helium in the local cloud along with the model predictions. Here $X_{\rm H} = n_{\rm H\,II}/(n_{\rm H\,I} + n_{\rm H\,II})$, and $X_{\rm He} = n_{\rm He\,II}/(n_{\rm He\,I} + n_{\rm He\,II})$. (Doubly ionized helium is assumed negligible.) Consistency of the HUT observation with the model predictions is apparent.

It should be noted that the similarity of the HUT neutral density ratio to the total cosmic ratio does not by itself rule out the possibility that both species are highly and *equally* ionized, as the HUT-allowed region of Figure 5 indicates. However, the principal theoretical problem with the preferentially ionized hydrogen picture has always been identifying a source to provide the necessary hydrogen ionization rate—adding a requirement for high helium ionization would only exacerbate the problem. Thus, the most straightforward interpretation is that the ionization of both species is modest, with that of helium slightly greater, and with both at levels sustainable by known ionizing sources. The HUT results thus remove completely the motivation for explanations like decaying massive neutrinos or very recent local supernovae to account for local ionization.

How can these results be reconciled with the earlier arguments in favor of high preferential hydrogen ionization? With regard to the backscatter experiments, the most likely explanation is that measurements within the solar system systematically underestimate the density of neutral hydrogen in the local ISM. It has long been recognized (Ripken & Fahr 1983) that charge exchange between interstellar protons and neutral hydrogen atoms at the heliopause (inside which solar particles and fields dominate over their interstellar counterparts) may cause a systematic depletion in the amount of neutral interstellar hydrogen atoms which flow into the inner solar system, where they are measured by the backscatter experiments. Ripken & Fahr predicted as much as 50% depletion in the observed hydrogen density, which is just the range required to bring the typical backscatter neutral ratios up to the cosmic value or above. In order to produce this degree of depletion of the neutral hydrogen density, this effect requires the initial

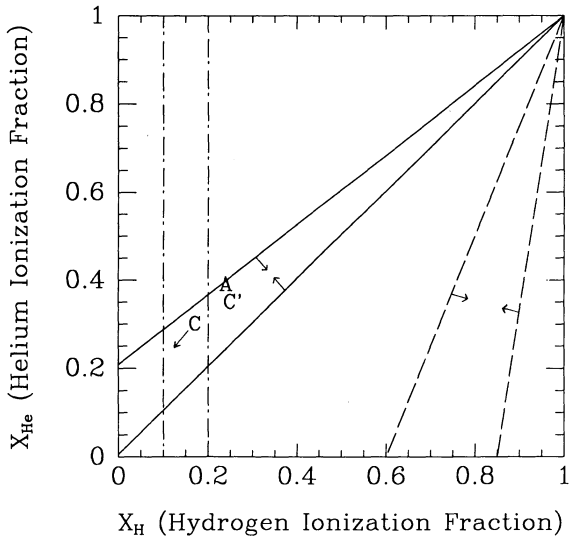

FIG. 5.—Hydrogen and helium ionization fractions in the local interstellar medium. The solid diagonal lines running from the lower left to the upper right on the figure bracket the HUT $\pm 1\ \sigma$ confidence limits on the neutral column ratio *integrated along the line of sight to G191-B2B*, assuming a total abundance ratio $N_{\rm H}/N_{\rm He} = 10$. The dashed lines to the right of the figure bound the region permitted by the representative backscatter measurements of Bertaux et al. (1985), *uncorrected for any systematic effects at the heliopause.* Points A and C are the ionization fractions *at the position of the Sun* in the corresponding models of Cheng & Bruhweiler (1990), while point C′ indicates the average ionization fractions *integrated along the line of sight from the Sun to the edge of the local cloud* for the model corresponding to point C.

The arrow pointing from point C toward lower ionization fractions for both species is an estimate of how the Cheng & Bruhweiler models would be affected by considering a higher neutral hydrogen column density to the edge of the cloud and a higher local neutral hydrogen density, as we infer from our observation of G191-B2B. Finally, the vertical dot-dashed lines bracket the 10%–20% range of interstellar hydrogen ionization necessary to produce a roughly 50% reduction in the neutral hydrogen density in the inner solar system through the charge-exchange mechanism of Ripken & Fahr (1983); a systematic effect of that order is required to reconcile the neutral density ratios observed in the backscatter data with the ratio observed by HUT.

hydrogen ionization (outside the solar system) to be ~10%–20%, just as predicted by Cheng & Bruhweiler (1990) and in good agreement with the HUT results (see Fig. 5).

The actual quantitative effectiveness of the Ripken & Fahr mechanism has been disputed (see Holzer 1989 for a recent review), and one explicit prediction—that the hydrogen temperature downwind in the inner solar system should be lower than the helium temperature—is in fact not observed (Bertaux et al. 1985). Nevertheless, some form of the Ripken & Fahr mechanism should be considered as a potential systematic error in the backscatter results; at the very least, it serves as an illustration of the many subtleties affecting the interpretation of the backscatter observations.

If in fact the backscatter-derived neutral hydrogen densities are systematically low by a factor of 2, then the typical backscatter-derived values can be combined with the HUT results and the model predictions to yield a fully consistent description of the densities and ionizations within the local cloud. In this picture, the *total* densities just outside the solar system are $n_{\rm H} \simeq 0.13$–$0.15\ {\rm cm}^{-3}$ and $n_{\rm He} \simeq 0.013$–$0.015\ {\rm cm}^{-3}$, with ionization fractions $X_{\rm H} \simeq 0.1$–0.2 and $X_{\rm He} \simeq 0.1$–0.35. These combine to yield *neutral* densities outside the solar system of $n_{\rm H\,I} \simeq 0.12\ {\rm cm}^{-3}$ and $n_{\rm He\,I} \simeq 0.01\ {\rm cm}^{-3}$, with the Ripken & Fahr effect reducing $n_{\rm H\,I}$ within the solar system to $\simeq 0.06\ {\rm cm}^{-3}$, as observed.

Toward the edge of the cloud, the ionization fractions of

both species gradually increase (Cheng & Bruhweiler 1990), so that the average ionization fractions along the path through the cloud are $X_H \simeq 0.25$ and $X_{He} \simeq 0.35$. Scaling from the neutral hydrogen column observed by HUT, we derive a *total* column toward G191-B2B of $N_H \simeq 2.2 \times 10^{18}$ cm^{-2} and conclude that the cloud extends ~ 5 pc in that direction.

With these parameters the average electron density in the cloud $n_e \simeq 0.03$ cm^{-3}, consistent with the low end of the electron density range inferred by Cox & Reynolds (1987) from the Mg I to Mg II column density ratio of Bruhweiler et al. (1984). It is consistent as well with the more recent Mg analysis of Frisch et al. (1990), as long as the local gas temperature is closer to the 7000 $\pm$ 200 K derived for the local hydrogen by Linsky et al. (1992), for example, than to the 11,750 K used by Frisch et al. (1990) in their analysis.

The remaining argument for preferential ionization of interstellar hydrogen in the local cloud (the discrepant *EXOSAT* vs. *Voyager* columns for HZ 43 and GD 153) is refuted by the EUV spectrum of HZ 43 also obtained with HUT, whose analysis we have completed just as this publication goes to press. The column densities permitted by the HUT HZ 43 observation (Kimble et al. 1992b) indicate that the low *EXOSAT* fluxes for HZ 43 cannot in fact be explained by an anomalous ratio of neutral helium to neutral hydrogen along the line of sight toward that star. Instead, the explanation must be either a calibration error in the *EXOSAT* spectroscopy or unexpected metal opacity in the stellar photosphere, though the very smooth grating spectra obtained with *EXOSAT* for HZ 43 (Paerels et al. 1986) show no obvious signs of such an opacity source.

5. SUMMARY

EUV observations of the hot DA white dwarf G191-B2B with the Hopkins Ultraviolet Telescope have provided the first high signal-to-noise ratio detection of neutral helium absorption in the local interstellar medium. In combination with the interstellar hydrogen column density derived from the same observation, the measured helium column yields a direct assessment of the ionization state of the low-density interstellar cloud surrounding the Sun. The observed neutral hydrogen–to–helium ratio of 11.6 $\pm$ 1.0 implies slightly higher ionization of helium than of hydrogen in the local material.

This result, like that of GJB, contradicts the widespread view that hydrogen is strongly and preferentially ionized in the local ISM, a view which had required the postulation of an intense additional ionizing source (such as decaying massive neutrinos) or transient ionization by a recent ($< 10^6$ yr ago) supernova within the local bubble. The relative ionization observed directly by HUT requires no such explanations; it is instead completely consistent with equilibrium ionization of the local cloud by known ionizing sources within the local bubble.

The HUT results suggest that backscatter determinations of the local interstellar gas densities systematically underestimate the neutral hydrogen density (perhaps due to some form of the Ripken & Fahr 1983 charge-exchange mechanism). If so, a consistent description of the local cloud can be obtained with total densities $n_H \simeq 0.13$–0.15 cm^{-3} and $n_{He} \simeq 0.013$–0.015 cm^{-3}, neutral densities $n_{H\,I} \simeq 0.12$ cm^{-3} and $n_{He\,I} \simeq 0.01$ cm^{-3}, ionization fractions $X_H \simeq 0.1$–0.2 and $X_{He} \simeq 0.1$–0.35 just outside the solar system, and an extent of $\simeq 5$ pc in the direction of G191-B2B. While this model cannot account for the seeming discrepancies between the *EXOSAT* and *Voyager* inferred column densities toward the hot DA white dwarfs HZ 43 and GD 153, our recently completed analysis of the HUT EUV spectrum of HZ 43 (Kimble et al. 1992b) suggests that the low fluxes reported by *EXOSAT* result from either a significant *EXOSAT* calibration error or unexpected photospheric opacity in the *EXOSAT* wavelength range, not from anomalous interstellar absorption.

Finally, if the intense 584 Å line emission from the G191-B2B vicinity reported by Green et al. (1990a) is real, it must come from the cool star companion G191-B2A. HUT upper limits to 584 Å line emission rule out G191-B2B or a surrounding nebula as the source.

It is a pleasure to thank the many individuals at the Johns Hopkins University Department of Physics and Astronomy and Applied Physics Laboratory for their contributions to the success of HUT. We are indebted also to the Spacelab Operations Support Group at Marshall Space Flight Center and to the crew of STS-35 for their many efforts to overcome the problems encountered during the flight. We also thank Pierre Bergeron for providing the G191-B2B model atmosphere, and David Finley and Detlev Koester for valuable discussions and for sharing their results in advance of publication. The Hopkins Ultraviolet Telescope project is supported by NASA contract NAS 5-27000 to The Johns Hopkins University.

APPENDIX

Before fitting models to the EUV spectrum to determine the interstellar absorbing columns, we first use the unfiltered FUV spectrum G191-B2B for some important calibrations. No astronomical calibration standards currently exist in the extreme ultraviolet. Insufficient observations have been made to date to establish an observational consensus, and no stellar model atmosphere can be used to establish a flux standard below 912 Å, because all targets beyond the solar system suffer from significant (and unknown) interstellar absorption.

It is therefore essential that some other approach be taken to determine with confidence the EUV sensitivity of the instrument in-flight. Pre- and postflight laboratory calibrations and a comparison of the G191-B2B model atmosphere with the unfiltered HUT far UV spectrum provide the necessary support. As described further in Davidsen et al. (1992), a postflight calibration of the HUT spectrograph was carried out in 1991 December, 1 year after the flight. When compared with the preflight calibration, which occurred 2 years before the flight, the postflight calibration revealed a small decline ($\sim 15\%$) in throughput in the EUV (at 584 Å) and a larger decline at longer wavelengths, reaching $\sim 35\%$ at 1777 Å, near the end of the HUT bandpass. This behavior, which we attribute to aging of the CsI photocathode, is identical to that seen for an earlier version of the HUT spectrograph. Our experience with that unit and limited monitoring of the flight spectrograph at one wavelength throughout the 3 year period involved suggest that the observed degradation occurred preflight and not during the 1 year period from *Astro-1* to the postflight calibration.

Comparison of the unfiltered HUT far-UV (first-order) spectrum with the model atmosphere calculation for G191-B2B described in the main text confirms this hypothesis. The HUT far-UV effective area curve derived from comparison to this model atmosphere is in remarkable agreement with the smoothed postflight calibration curve (with a mean difference of $<1\%$, and an rms dispersion of only 6.7% in the ratio of the two curves). This agreement forms a firm basis for the assumptions underlying our EUV analysis: (1) that the postflight spectrograph calibration provides an accurate measure of the in-flight EUV sensitivity of the instrument (recall that the decline in the EUV was modest [15%] in any case), and (2) that the adopted stellar parameters and model atmosphere calculation for G191-B2B are accurate.

Another calibration required is for the transmission of the aluminum filter. An inflight determination is particularly important here. The filter is mounted outside the sealed, evacuated spectrograph and was exposed to less well controlled environments after the landing of the shuttle than before. It is therefore not clear that the postflight measurements (which showed a drop in throughput of 20% at 584 Å) should be preferred for this component.

Instead we obtain a measurement of the in-flight filter transmission in the 420–450 Å range through a direct comparison of the filtered and unfiltered HUT spectra for G191-B2B, and an estimate of the in-flight 584 Å transmission through a comparison of filtered and unfiltered observations of the 584 Å airglow line under similar geographic conditions. The short-wavelength region of the HUT unfiltered spectrum, nominally 840–900 Å in first order, is in fact completely dominated for G191-B2B by second-order 420–450 Å radiation. The intrinsic stellar spectrum is 3 times stronger at 435 Å than at 870 Å, the efficiency of HUT is comparable at the two wavelengths, and the attenuation of the 870 Å signal by interstellar absorption is 60 times stronger than at 435 Å for a neutral hydrogen column of 1×10^{18} cm^{-2} and nearly 4000 times stronger for a hydrogen column of 2×10^{18} cm^{-2}. The column we ultimately derive is closer to the latter figure, confirming the assumption of a negligible first-order 840–900 Å contribution to the observed signal.

Similarly, the declining throughput of the instrument at short wavelengths yields an upper limit of a few percent on the strength of the third- and higher order signals compared with the second-order 420–450 Å. The unfiltered spectrum does require correction ($\sim 30\%$) for scattering from the strong far-UV signal longward of 912 Å (the scattering level was determined from observations of stars of similar spectral shape, whose EUV flux is completely cut off by higher interstellar opacity). With the scattering and (small) dark count corrections made, the comparison of the unfiltered and filtered G191-B2B spectra yields a 435 Å in-flight transmission of 20.4%, down by 10% from the preflight value of 22.6%.

At 584 Å, comparison of the airglow line strength observed during the only daytime use of the aluminum filter with the unfiltered signal seen during an observation with similar geographic conditions yields a decline of $15\% \pm 10\%$ for the transmission at this wavelength. Given the uncertainty in the assumption of identical airglow intensity for the two observations, we take this comparison simply as an encouraging confirmation of a modest decline in filter transmission and adopt an in-flight transmission curve that is a flat 10% below the preflight curve at all wavelengths.

One other calibration issue must be addressed: the strength of the third-order signal near the second-order 504 Å edge. As noted above, the third-order contribution to the observed spectrum is very uncertain at short wavelengths. The third-order wavelength overlying the second-order 504 Å is 336 Å; no preflight calibration data for the instrument are available shortward of 460 Å. Furthermore, the stellar flux will presumably deviate from the pure hydrogen model by more and more as the wavelength decreases toward the *EXOSAT* range, where the flux is known to lie significantly below the pure hydrogen prediction. Thus, no rigorous determination of the third-order contribution to the relevant wavelength interval can be made.

However, we can firmly bracket the third-order signal and derive a reasonable estimate of its level. The maximum plausible third-order signal is determined in the following manner. Throughput of the instrument can be extrapolated from the wavelength range covered by the laboratory calibration by assuming standard values for the efficiencies of the various components: the iridium-coated primary mirror, the osmium-coated holographic grating, and the CsI-coated microchannel plate detector. The largest uncertainty here would be expected to be the groove efficiency of the diffraction grating. However, for all wavelengths measured in the laboratory, we find that the intensity ratios of various diffracted orders can be well fit by the theoretically predicted efficiencies of the sinusoidal grooves produced by conventional holographic ruling techniques. The third-order efficiency for the best-fitting groove depth reaches its maximum in the 336 Å region. As the pure hydrogen model atmosphere prediction is also presumably greater than or equal to the actual stellar flux in this region, the product of the extrapolated instrumental throughput and the hydrogen model flux should provide an upper bound to the potential contribution of third order to the spectrum.

Two lines of argument indicate that the actual third-order contribution does indeed lie below this bound. First, in the region covered by the laboratory calibration, the instrumental throughput declines more rapidly toward shorter wavelengths than the component "standard values" would predict, indicating that some component is underperforming at the shortest wavelengths. Second, when the upper bound on the third-order throughput is used in fitting the second-order 479–529 Å region, the resulting best fit systematically exceeds the observed signal markedly for regions longward of the fitted interval (second-order wavelengths from 540 to 600 Å).

A firm lower bound on the third-order contribution to the observed spectrum is obviously that it is ≥ 0. A reasonable estimate to the true value is obtained by suppressing the upper limit to the third-order throughput by an arbitrary factor until the best-fitting parameters for the 479–529 Å range no longer overpredict the observed spectrum at longer wavelengths. We employ this suppression factor in deriving our best-fitting model parameters.

Any plausible contribution of the third-order signal to the total observed spectrum in the 479–529 Å interval is thus $\leq 15\%$. The full range of uncertainty described above therefore has very little effect on the ultimate results. Compared with the column densities derived from the "best estimate" third-order contribution, the results using the upper and lower bounds described above differ by $<4\%$ for the hydrogen column and $<2\%$ for the helium column.

REFERENCES

Aller, L. H. 1987, in Spectroscopy of Astrophysical Plasmas, ed. A. Dalgarno & D. Layzer (Cambridge: Cambridge Univ. Press), 89
Baldwin, J. A., Ferland, G. J., Martin, P. G., Corbin, M. R., Cota, S. A., Peterson, B. M., & Slettebak, A. 1991, ApJ, 374, 580
Bertaux, J. L., Lallement, R., Kurt, V. G., & Mironova, E. N. 1985, A&A, 150, 1
Bruhweiler, F. C., & Feibelman, W. A. 1992, preprint
Bruhweiler, F. C., & Kondo, Y. 1982, ApJ, 259, 232
Bruhweiler, F. C., Oegerle, W., Weiler, E., Stencel, R., & Kondo, Y. 1984, in IAU Colloq. 81, The Local Interstellar Medium, ed. Y. Kondo, F. C. Bruhweiler, & B. D. Savage (Washington: NASA CP-2345), 64
Bruhweiler, F. C., & Vidal-Madjar, A. 1987, in Exploring the Universe with the *IUE* Satellite, ed. Y. Kondo (Dordrecht: Reidel), 467
Chassefière, E., Bertaux, J. L., Lallement, R., & Kurt, V. G. 1986, A&A, 160, 229
Cheng, K.-P., & Bruhweiler, F. C. 1990, ApJ, 364, 573
Cox, D. P., & Reynolds, R. J. 1987, ARA&A, 25, 303
Cruddace, R., Paresce, F., Bowyer, S., & Lampton, M. 1974, ApJ, 187, 497
Davidsen, A. F., Kimble, R. A., Durrance, S. T., Bowers, C. W., & Long, K. S. 1991a, in Extreme Ultraviolet Astronomy, ed. R. Malina & S. Bowyer (New York: Pergamon), 427
Davidsen, A. F., et al. 1991b, Nature, 351, 128
Davidsen, A. F., et al. 1992, ApJ, 392, 264
Finley, D. S., & Koester, D. 1992, private communication
Frisch, P. C., Welty, D. E., York, D. G., & Fowler, J. R. 1990, ApJ, 357, 514
Green, J., Bowyer, S., & Jelinsky, P. 1990a, ApJ, 353, 612
Green, J., Jelinsky, P., & Bowyer, S. 1990b, ApJ, 359, 499 (GJB)
Hedin, A. E. 1987, J. Geophys. Res., 92, 4649
Heise, J., Paerels, F. B. S., Bleeker, J. A. M., & Brinkman, A. C. 1988, ApJ, 334, 958
Holberg, J. B. 1984, in IAU Colloq. 81, The Local Interstellar Medium, ed. Y. Kondo, F. C. Bruhweiler, & B. D. Savage (Washington: NASA CP-2345), 91
Holberg, J. B., Ali, B., Carone, T. E., & Polidan, R. S. 1991, ApJ, 375, 716
Holzer, T. E. 1989, ARA&A, 27, 199
Jelinsky, P., Bowyer, S., & Basri, G. 1988, in A Decade of UV Astronomy with IUE—A Celebratory Symposium, ed. E. J. Rolfe (Noordwijk: ESA) (ESA SP-281), 2, 235
Kimble, R. A., Davidsen, A. F., Long, K. S., Bowers, C. W., Kriss, G. A., Finley, D. S., & Koester, D. 1992a, in preparation
Kimble, R. A., Davidsen, A. F., Long, K. S., & Feldman, P. D. 1992b, ApJ, submitted
Koester, D. 1989, ApJ, 342, 999
Koester, D., Vauclair, G., Dolez, N., Oke, J. B., Greenstein, J. L., & Weidemann, V. 1985, A&A, 149, 423
Linsky, J. L., et al. 1993, ApJ, 402, 694
Lowry, H. F., Tomboulian, D. H., & Ederer, D. L. 1965, Phys. Rev., 137, A1054
Marr, G. V., & West, J. B. 1976, Atomic Data Nucl. Data Tables, 18, 497
Paerels, F. B. S., Bleeker, J. A. M., Brinkman, A. C., Gronenschild, E. H. B. M., & Heise, J. 1986, ApJ, 308, 190
Paerels, F. B. S., & Heise, J. 1989, ApJ, 339, 1000
Peimbert, M., Ukita, N., Hasegawa, T., & Jugaku, J. 1988, PASJ, 40, 581
Reilman, R. F., & Manson, S. T. 1979, ApJS, 40, 815
Ripken, H. W., & Fahr, H. J. 1983, A&A, 122, 181
Routly, P. M. 1972, Publ. US Naval Obs., 2d Ser., 20, part 6
Sciama, D. W. 1991, A&A, 245, 243
Sion, E. M., Bohlin, R. C., Tweedy, R. W., & Vauclair, G. P. 1992, ApJ, 391, L29
Slavin, J. D. 1989, ApJ, 346, 718
Spitzer, L. 1978, Physical Processes in the Interstellar Medium (New York: John Wiley), 105
Turck-Chieze, S., Cahen, S., Casse, M., & Doom, C. 1988, ApJ, 335, 415
Vennes, S., Chayer, P., Fontaine, G., & Wesemael, F. 1989, ApJ, 336, L25
Vennes, S., Chayer, P., Thorstensen, J. R., Bowyer, S., & Shipman, H. L. 1992, ApJ, 392, L27